Science of the Total Environment 441 (2012) 117–124

Contents lists available at SciVerse ScienceDirect

Science of the Total Environment

journal homepage: www.elsevier.com/locate/scitotenv

Genotoxic effects of copper oxide nanoparticles in Neuro 2A cell cultures

François Perreault [a,b], Silvia Pedroso Melegari [a], Cristina Henning da Costa [a], Ana Letícia de Oliveira Franco Rossetto [a], Radovan Popovic [b], William Gerson Matias [a,*]

[a] Laboratório de Toxicologia Ambiental, LABTOX-Depto. de Engenharia Sanitária e Ambiental, Universidade Federal de Santa Catarina, Campus Universitário, CEP: 88040-970, Florianópolis, SC, Brazil
[b] Department of Chemistry, University of Quebec in Montreal, C.P. 8888, Succ. Centre-Ville, Montreal, Quebec, Canada, H3C 3P8

HIGHLIGHTS

- Particles formed large agglomerates of over 300 nm in the medium.
- CuO nanoparticles are cytotoxic and genotoxic for Neuro 2A cells.
- CuO NPs induce significant lipid peroxidation and DNA fragmentation at 25 mg l^{-1}.
- CuO nanoparticles increase micronucleus frequency at 12.5 mg l^{-1}.
- Genotoxic effects of CuO NPs are an important aspect of its toxicological risk.

ARTICLE INFO

Article history:
Received 30 May 2012
Received in revised form 25 September 2012
Accepted 25 September 2012
Available online 6 November 2012

Keywords:
Nanotoxicology
Micronucleus
DNA methylation
Lipid peroxidation
Cytotoxicity

ABSTRACT

Copper oxide nanoparticles (CuO NPs) are used for their biocide potential however they were also shown to be highly toxic to mammalian cells. Therefore, the effects of CuO NPs should be carefully investigated to determine the most sensitive processes for CuO NP toxicity. In this study, the genotoxicity of CuO NPs was investigated *in vitro*, using the mouse neuroblastoma cell line Neuro-2A. Genotoxic effects related to DNA fragmentation, DNA methylation and chromosomal damage, as well as lipid peroxidation, were investigated and compared to cytotoxic effects, measured by the mitochondrial reduction of 3-(4,5-dimethylthiazol-2-yl)-2,5-diphenyltetrazolium bromide into formazan. Based on mitochondrial activity, CuO NPs were found to be cytotoxic. At the highest concentration tested (400 mg l^{-1}), 63% of cell viability was found in Neuro-2A cells after 24 h of treatment to CuO NPs. CuO NPs were also found to induce DNA fragmentation, lipid peroxidation and micronucleus formation. The micronucleus assay was the most sensitive to evaluate CuO NP genotoxicity and micronucleus frequency was increased significantly at 12.5 mg l^{-1} CuO NPs after 24 h of treatment. At this concentration, no significant change of cell viability was found using the mitochondrial activity assay. These results highlight the important risk of genotoxic effects of CuO NPs and show that genotoxicity assays are a sensitive approach to evaluate the risk of CuO NP toxicity.

1. Introduction

Nanotechnology is a new promising field with potential applications in domestic, industrial and biomedical products (Peralta-Videa et al., 2011). Due to the growing number of applications, there is an increasing risk of human and environmental exposure to nanomaterials. Their potential toxicological impacts are still a matter of investigation and our actual knowledge on the effects of nano-sized contaminants on biological systems remains incomplete (Singh et al., 2009; Skocaj et al., 2011). These effects need to be carefully assessed in order to provide a scientific basis for a safe development of nanotechnologies.

Copper oxide nanoparticles (CuO NPs) possess biocide properties interesting for applications in antimicrobial textiles, paints and plastics (Ren et al., 2009; Dastjerdi and Montazer, 2010; Delgado et al., 2011). However, CuO NPs were found to be highly toxic compared to other carbon or metal oxide nanomaterials (Karlsson et al., 2008; Wang et al., 2011). Due to their small size, NPs may cross biological barriers to reach different organs and, according to their size and surface properties, accumulation of metal NPs was previously observed in all the different organs *in vivo* (for a review, see Li and Chen, 2011). Metallic NPs such as MnO_2 NPs or gold NPs were found to accumulate in the brain of rats and mice, respectively (Lasagna-Reeves et al., 2010; Oszlanczi et al., 2010). CuO NP treatment is known to induce a disruption of the blood–brain barrier *in vivo* in mice and rats (Sharma et al., 2010). Moreover, under *in vitro* conditions, CuO NPs were also found to induce toxic effects in different types of neuronal cells such as the human SH-SY5Y neuroblastoma and H4 neuroglioma cells (Li et al., 2007; Chen et al., 2008). However, several aspects of CuO NP toxicity on such cellular systems remain unknown. Genotoxicity of nanomaterials is of particular concern since an alteration of the genetic material may favor cancer development or fertility impairment (Singh

* Corresponding author. Tel.: +55 48 37217742; fax: +55 48 37219823.
E-mail address: will@ens.ufsc.br (W.G. Matias).

0048-9697/$ – see front matter © 2012 Elsevier B.V. All rights reserved.
http://dx.doi.org/10.1016/j.scitotenv.2012.09.065

et al., 2009). Nanomaterials were shown to induce DNA alterations by two pathways: *via* direct association with DNA strands for NPs of small (1–2 nm) diameter (Tsoli et al., 2005), or mediated by oxidative stress induced by NPs (Shukla et al., 2011). Previous studies, using human lung epithelial cells A549 indicated that CuO NPs may have deleterious effects on DNA integrity (Karlsson, 2010; Ahamed et al., 2010). However, further investigations are required to provide a better understanding of the risk of genotoxicity of CuO NPs.

Genotoxic effects of contaminants may be induced by different pathways, such as direct DNA damage (Zhivotosky and Orrenius, 2001; Karlsson, 2010) or by chromosomal damage caused by an alteration of DNA integrity or the disruption of cell division processes (Fenech, 2000). Indirect processes may also be implicated in genotoxic effects of contaminants. For example, epigenetic changes such as methylation of cytosine (dC) into 5-methyldeoxycytosine (m^5dC) may alter gene expression and lead to carcinogenesis (Zukiel et al., 2004). Change in the m^5dC:dC ratio, in addition to favoring mutagenesis by m^5dC deamination to thymine, can trigger the activation of proto-oncogenes or the inactivation of tumor suppression genes (Gonzalgo and Jones, 1997). Finally, cellular stress may lead to genotoxic effects *via* oxidation by-products such as malondialdehyde (MDA), a mutagenic and carcinogenic by-product of lipid peroxidation (Marnett, 1999).

In this report, CuO NP genotoxic effects were evaluated *in vitro* and compared with cytotoxic effects to better understand the risk of CuO NP exposure. The Neuro-2A (N2A) mouse neuroblastoma cell line was used as a model to determine the potential toxicological effect of CuO NP accumulation in the brain. The change of different toxicity endpoints was compared to identify the most sensitive processes in CuO NP action at the cellular level.

2. Materials and methods

2.1. Cell culture

The N2A mouse neuroblastoma cell line was obtained from the National Museum of Nature, Paris, France (European Collection of Cell Cultures cat. no. 89121404; PortonDown, UK). Cells were grown in RPMI-1640 medium supplemented with 10% fetal bovine serum, 2 mM glutamine, 1 mM sodium pyruvate, 50 mg ml^{-1} streptomycin and 50 U ml^{-1} penicillin (all reagents were obtained from Sigma-Aldrich, Lyon, France). The culture was maintained at 37 °C in a humidified air:CO_2 (95:5) atmosphere (Humpage et al., 2007).

2.2. Preparation of the NP suspension

CuO nanopowder was obtained from MTI corporation (Richmond, CA) and, according to the manufacturer, had an average size of 30–40 nm and a purity higher than 99%. Nanopowder was exposed to UV illumination for 30 min before use to avoid bacterial contamination. Stock CuO NP suspension (4 mg ml^{-1}) was prepared in sterile nanopure water and sonicated 2×150 s at 50 W, with 10 s of vortex between each sonication. CuO NPs were stabilised using albumin in a protocol modified from Bihari et al. (2008), as this protein is already present in the culture media, has a high affinity to NPs and a low effect on biochemical reactions (Bihari et al., 2008). Stabilisation of NPs by albumin is a widely used approach to stabilise NPs in biological medium and is used by the NANOGENOTOX joint action as a standard operation procedure (Jensen et al., 2011). After the two initial sonication steps, bovine serum albumin was added to a final concentration of 1.5 mg ml^{-1} and the suspension was sonicated a third time for 60 s at 37.5 W. The CuO NP suspension was prepared just before treatment.

Raw nanopowder was visualized by scanning electronic microscopy (SEM) to determine initial particle size. CuO NPs were first dispersed in nanopure water, deposed on the sample holder and left to dry. Samples were covered with a 5 nm gold film and desiccated for 3 days. Analysis was realized on a JEOL JSM-6701F microscope at the Laboratório Central de Microscopia Eletrônica (UFSC, Brazil). CuO NPs were characterized in the RPMI media used for treatments using a ZetaPlus particle sizer (Brookhaven Instruments Corporation, NY). Particle size distribution was determined by dynamic light scattering and zeta potential of NPs by the electrophoretic mobility method. NP size and shape were also verified by transmission electronic microscopy (TEM). For TEM analysis, a drop of NP suspension (1 mg ml^{-1}) was placed on a formvar-coated copper grid and, after 1 min, the media was removed with a Whatman filter paper. Samples were visualized using a FEI Tecnai 12 120 kV microscope and pictures taken with a Gatan 792 Bioscan 1 k×1 k Wide Angle Multiscan CCD camera.

2.3. NP treatments

N2A cells (10^5cells ml^{-1}) were first seeded in 6, 24 or 96-well microplates (according to the assay used) with 5% of CO_2 at 37 °C during 24 h. Then, the medium was removed and cells were exposed to CuO NP concentrations from 6.25 to 400 mg l^{-1} diluted in RPMI 1640 without any supplements to limit cell proliferation. N2A cells were exposed during 24 h to CuO NPs, in 5% of CO_2 at 37 °C in the dark.

2.4. Mitochondrial activity assay

Cell viability was determined with the mitochondrial activity assay by the measure of 3-(4,5-dimethylthiazol-2-yl)-2,5-diphenyltetrazolium bromide (MTT) reduction. N2A cells were exposed to CuO NPs in 96-well plates during 24 h. At the end of the treatment, the supernatant was discarded and 200 µl of MTT (0.5 mg ml^{-1} in RPMI-1640) was added and cells were incubated for 2 h. Then, the MTT solution was discarded and 200 µl of dimethyl sulfoxide was added to each well to dissolve the formazan crystals formed. Absorbance was read at 560 nm using a BioTek EL 3 800 microplate reader (BioTek Instruments, Winooski, VT). Reference wells were used to correct for any absorbance of CuO NPs at 560 nm. From the MTT results, the EC_{10} value was calculated by fitting a 4 parameter sigmoidal equation (Hill-slope model).

Interactions between CuO NPs and the MTT assay was evaluated by the same protocol as described without the N2A cells. For each CuO NP concentration used, the NPs were incubated in RPMI media supplemented with MTT solution for 2 h at 37 °C. The absorbance at 560 nm was used to monitor MTT reduction into formazan by NPs. Reference wells were used to correct for any absorbance of CuO NPs at 560 nm.

2.5. Lipid peroxidation

MDA quantification was performed according to Matias and Creppy (1998), with modifications. N2A cells were exposed to CuO NPs (12.5, 25, 50 and 100 mg l^{-1} in RPMI-1640) in 24-well plates during 24 h. At the end of the exposition, the media was discarded; the cells were collected in 500 µl PBS and centrifuged at 1000 *g* for 5 min. PBS was discarded and 150 µl of SET buffer (0.1 M NaCl, 20 mM EDTA, 50 mM Tris–HCl, pH 8.0) was added. The samples were vortexed and 20 µl was taken to measure the protein content using the Bradford assay (Bradford, 1976). Then, 25 µl of 7% sodium dodecyl sulfate, 300 µl of 0.1 M HCl, 40 µl of 1% phosphotungstic acid and 300 µl of 0.67% thiobarbituric acid (TBA) were added to each sample and vortexed. Samples were incubated at 90 °C for 1 h in the dark, and then cooled in ice bath for 15 min. 300 µl of n-butanol was added to each sample and vortexed. Samples were centrifuged at 3000 *g* for 10 min and the n-butanol phase containing the MDA-TBA adduct was separated and quantified using a HP1050 HPLC system (Hewlett Packard, Barueri, Brazil) equipped with Supelcosil LC-18 column (250×4.6 mm, 5 µm). The mobile phase consisted of methanol:water 40:60 (v/v), pH 8.4. The flow rate was kept at 0.5 ml min^{-1}, and the injection volume was 50 µl. Detection was done using a Programmable Fluorescence Detector HP 1064A. The excitation and emission wavelengths were of 515 and

553 nm, respectively. MDA calibration curve was prepared with eight samples of standard MDA concentrations varying between 7.5 and 6×10^7 nM, prepared the same way as samples to form the MDA–TBA complex. Quantification of MDA–TBA was done in relation to the total protein content.

2.6. DNA extraction and genotoxicity assay

N2A cells (10^5 cells ml^{-1}) were seeded in 6-wells microplates and treated with CuO NPs (12.5, 25, 50 and 100 mg l^{-1} in RPMI-1640). A positive control has been performed in parallel using cyclophosphamide (1 mg l^{-1}). After 24 h of treatment, the culture medium was removed and the cells were harvested by scraping with 1 ml of PBS. DNA was extracted from control and treated cells using a Wizard Genomic DNA Purification Kit (Promega) according to the manufacturers' protocol. Total DNA was quantified using the ratio of absorbance at 260/280 nm (adapted from Kouadio et al., 2007).

2.7. DNA fragmentation assay in agarose gel electrophoresis

Qualitative evaluation of DNA fragmentation was done by agarose gel electrophoresis. 10 μg of purified DNA of N2A cells was carried out by electrophoresis (MSMIDI 738, Biosystems) in 1.5% agarose gel prepared in TBE buffer (Tris 44.5 mM, boric acid 44 mM and EDTA 50 mM). DNA migration was carried out in electrophoresis buffer under 70 V during 2 h. At the end of the migration, the gel was incubated in TBE buffer containing 0.02 mg ml^{-1} ethidium bromide and DNA was revealed under UV light using a transiluminator (LTB-ST Loccus Biotecnologia, SP-Brazil). DNA gel images were captured with a digital camera (L-PIX Loccus Biotecnologia, SP-Brazil) and analyzed with the Image J software (National Institutes of Health, Bethesda, MD) (Slade et al., 2009).

2.8. DNA methylation

For m^5dC quantification, 10 μg of purified DNA from exposed N2A cells was dissolved in 10 μl of nanopure water and incubated at 100 °C for 2 min. Then, 1 μl of 250 mM potassium acetate buffer (pH 5.4), 1 μl of 10 mM zinc sulfate, and 10 μl of nuclease P1 (0.5 U ml^{-1}) was added and samples were kept at 37 °C overnight. After incubation, the samples were treated with 2 μl of 0.5 M Tris–HCl (pH 8.3), plus 2 μl of the buffer containing 0.31 U ml^{-1} alkaline phosphatase. Samples were incubated at 37 °C for 2 h. DNA bases composition was analyzed on a HP1050 HPLC system (Hewlett Packard, Barueri, Brazil) equipped with a HP1050 Series Variable Wavelength Detector and a Agilent Zorbax SB-Phenyl column (250×4.6 mm^2, 5 μM). Elution was carried out with 6.5 mM $(NH_4)H_2PO_4$ pH 3.95 and 4% methanol (v/v) at a flow rate of 1 ml min^{-1}. Eluates were monitored at 254 nm. The samples were diluted to 1:4 and the injection volume was 20 μl. Standard DNA bases (dC, dT, dG, dA; 100 μg ml^{-1} each) and m^5dC (10 μg ml^{-1}) were used for quantification. The results in μg ml^{-1} were used to calculate the % rate of m^5dC as compared to $[m^5dC+dC]\times100$.

2.9. Micronucleus assay

Cytochalasin B-blocked micronucleus assay was performed as described in Ouanes et al. (2003), with some modification. For micronucleus assay, N2A cells (10^5 cells ml^{-1}) were cultivated for 24 h in 24-well plates, and then exposed to CuO NP, with RPMI 1640 medium as negative control and cyclophosphamide (1 mg l^{-1}) as positive control. Cytochalasin B (Cyt-B, 5 μg ml^{-1}) was subsequently added to the treated cultures 6 h after start of treatment for a further 18 h incubation period. Cells were harvested after 24 h treatment, transferred to 0.075 M KCl for a mild hypotonic treatment and then immediately centrifuged at 5000 *g* for 5 min. Supernatant was discarded and cells were fixed in 250 μl methanol/acetic acid 3:1 (v:v) for 20 min. Fixed cells were spread on glass slides and dried for 30 min. Staining was done with acridine orange/ethidium bromide and slides were analyzed at 400× magnification using a fluorescent microscope (Olympus BX40, Japan). One thousand binucleated cells were assessed per slide.

2.10. Data analysis and statistics

All experiments were done in three replicates. For toxicity thresholds (EC_{50} and EC_{10}), toxicity data were fitted with a 4 parameter sigmoidal equation (Hill-slope model) using the GraphPad Prism software (GraphPad Software, Inc., La Jolla, CA). Results were compared using an ANOVA followed by a Tukeys' test. Results were considered significant for $p<0.05$.

3. Results

3.1. CuO NP aggregation in the media

SEM microscopy visualization of CuO NPs indicated that CuO NPs were agglomerated after being dispersed in nanopure water. Indeed, individual CuO particles had a diameter between 70 and 100 nm while larger agglomerates of several hundred nanometers were observed (Fig. 1A). After sonication and suspension in the culture media, TEM micrographs showed a CuO core of 102 ± 34 nm located inside a less electronically dense material that can be attributed to albumin proteins as described in Bihari et al. (2008). The protein–NPs complex had a total average size of 356 ± 70 nm (Fig. 1B). These values were in agreement with dynamic light scattering analysis, which indicated a NPs size distribution in liquid media mostly centered around 300 nm (99.1% of all particles), with some agglomerate formation with micron-sized diameter (2.1 μm) (Fig. 2). Therefore, in the culture media, particles formed complexes larger than the nanoscale range (1–100 nm). Similarly to the observation of Bihari et al. (2008), formation of a protein layer around CuO NPs decreased particle surface charge from -46.05 ± 3.54 to -6.04 ± 1.00 mV.

3.2. MTT assay

The MTT mitochondrial activity assay was used to evaluate the effect of CuO NP treatment on N2A cell viability. This approach was evaluated for any interactions between NPs and the MTT assay and it was concluded that CuO NPs alone do not induce a significant reduction of MTT into formazan, which validate this assay for evaluating their effect on N2A cells (Fig. 3, insert). After 24 h of N2A treatment to CuO NPs, low concentrations (6.25 and 12.5 mg l^{-1}) were found to increase mitochondrial activity while higher concentrations decreased mitochondrial activity (Fig. 3). At the highest concentration tested (400 mg l^{-1}), mitochondrial activity was decreased to 63.1 ± 11.7% of control sample. Based on the MTT results, EC_{10} value of 20.84 ± 2.46 mg l^{-1} (2.3–189.2 mg l^{-1}, 95% confidence interval) was found by fitting a 4 parameter sigmoidal equation to the experimental data. However, this toxicity threshold value should be considered with care since the concentration range tested did not cover the complete dose–response curve and therefore results in a poor fit of the dose–response curve ($R^2=0.72$) (Sebaugh, 2010). Similarly, EC_{50} value was not calculated since the concentration range used in this study did not provide a toxic response lower than 63%.

3.3. Lipid peroxidation

Exposition of N2A cells to CuO NP treatments resulted in oxidative stress, measured by the formation of MDA. After 24 h of treatment, CuO effect on MDA content was significant from a CuO concentration of 25 mg l^{-1} ($p<0.05$) or higher. CuO NP treatment at 25 mg l^{-1} increased the MDA content at 217% of the negative control value, while this value reached 543% for 100 mg l^{-1} CuO NPs (Fig. 4). In

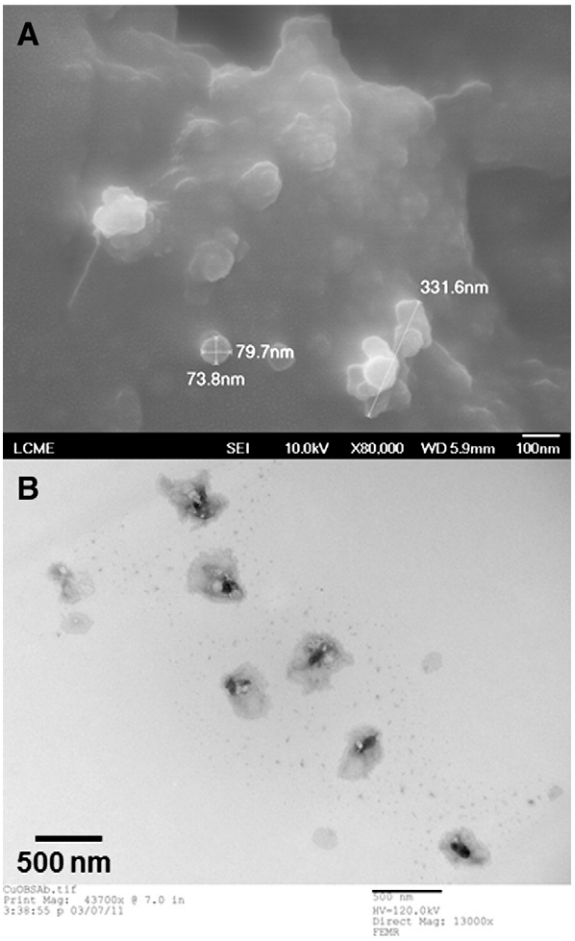

Fig. 1. A. SEM microscopy picture of CuO NPs in water. B. TEM microscopy picture of CuO NPs in the culture media.

comparison, cyclophosphamide treatment, which was used as a positive control, increased the MDA content to 333% of the control value.

3.4. DNA fragmentation

Agarose gel electrophoresis of total DNA extracted from N2A cells after 24 h of CuO NP treatments indicated the presence of DNA fragmentation in all treatments (Fig. 5A). CuO NP exposure, compared

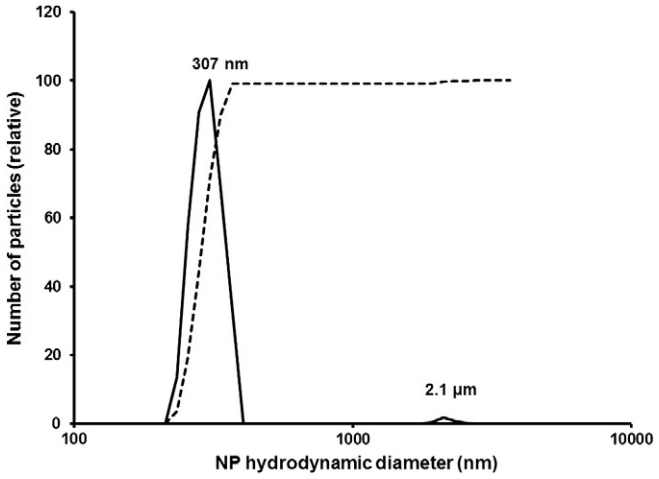

Fig. 2. Size distribution of CuO NPs in the culture media. Bold line indicates the size distribution of NPs. The dashed line indicates the cumulative total fraction of particles.

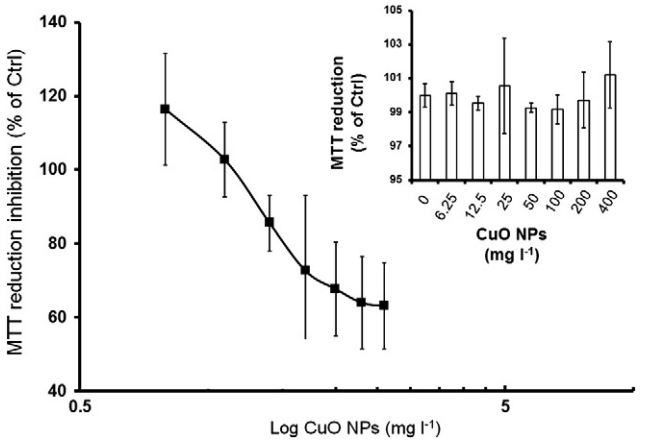

Fig. 3. Change of N2A cell viability after 24 h of exposure to CuO NPs. Cell viability was determined using the mitochondrial MTT assay. Inset: change in MTT reduction induced by CuO NPs alone. Data are presented as mean ± standard deviation (n = 3).

to the negative control (untreated sample) increased DNA fragmentation up to a concentration of 50 mg l^{-1}, while exposure of N2A cells to 100 mg l^{-1} reduced DNA fragmentation. Using the image analysis software Image J, DNA fragmentation was quantitatively compared to the control (Fig. 5B). At 50 mg l^{-1} CuO NPs, DNA fragmentation was increased by 30% compared to control. This effect was similar to the effect of the positive control toxicant cyclophosphamide (1 mg l^{-1}). DNA fragmentation was significantly different from the negative control from a concentration of 25 mg l^{-1} CuO NPs.

3.5. DNA methylation

Methylation of dC into m^5dC was evaluated by the change in the m^5dC/dC ratio. Negative control N2A cells had an m^5dC/dC ratio of 0.38%, which is close to previous findings for this cell line (Perreault et al., 2011). However, CuO NPs treatment did not show any significant change of m^5dC/dC ratio even at 100 mg l^{-1} (Fig. 6). Changes in the m^5dC/dC ratio induced by CuO NPs were less than 1%, which may indicate that CuO NPs do not alter DNA methylation rate *in vitro*. It should be noted that the positive control, cyclophosphamide, did not result in a significant change of DNA methylation either. Therefore, from such results, no specific conclusions may be done for CuO NPs effect on DNA methylation processes in N2A cells.

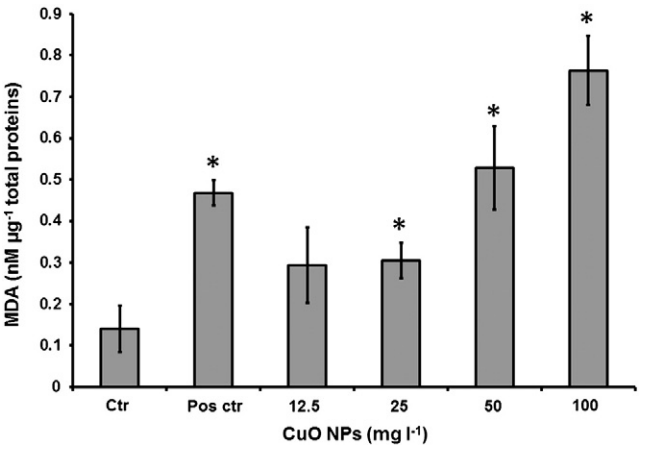

Fig. 4. MDA concentrations in N2A cells after a 24 h exposure to 12.5, 25, 50 and 100 mg l^{-1} CuO NPs. Cyclophosphamide was used as a positive control (Pos Ctr). Data are presented as mean ± standard deviation (n = 3).

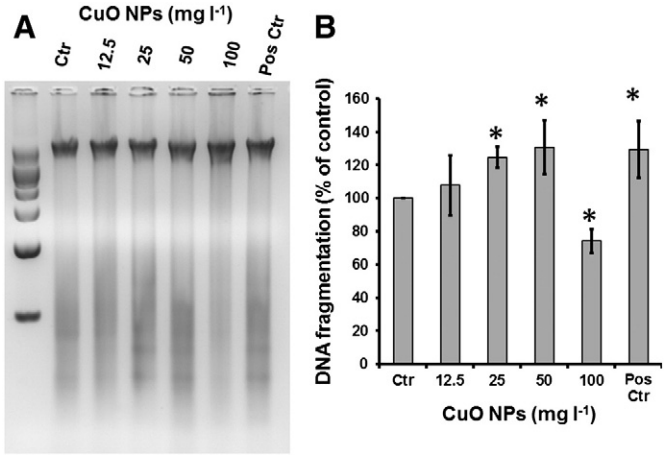

Fig. 5. DNA fragmentation in N2A cells after a 24 h exposure to 12.5, 25, 50 and 100 mg l^{-1} CuO NPs. Cyclophosphamide was used as a positive control (Pos Ctr). A. Agarose gel electrophoresis of Neuro-2A DNA extracts. B. Image analysis of DNA band intensity. Data are presented as mean ± standard deviation (n = 3).

3.6. Micronucleus formation

Chromosomal damage induced by CuO NPs was evaluated using the cytochalasin B-blocked micronucleus assay, in which cell division is blocked to allow the numbering of dividing cells only (binucleated cells, Fig. 7A). In the untreated cells, micronucleus frequency was less than two per 1000 binucleated cells (Fig. 8). CuO NP treatments increased significantly the frequency of micronucleus formation at the lowest concentration tested (12.5 mg l^{-1}, $p<0.05$) and reached as high as 15 micronuclei per 1000 binucleated cells for 100 mg l^{-1} CuO NPs (Fig. 8). CuO NPs treatment induced micronuclei of both type I (micronucleus smaller than 1/4 the size of the nucleus, Fig. 7B) and type II (micronucleus between 1/4 and 1/2 the size of the nucleus, Fig. 7C and D). Type I micronuclei are considered as an indicator of a clastogenic effect and contain small chromosome fragments, while Type II micronuclei are considered as indicating aneugenic effects and contain whole chromosomes (Tinwell and Ashby, 1991; Hashimoto et al., 2010). Type I micronuclei were more frequent in all CuO NPs treatment, with a frequency between 70 and 80%, and did not increase with increasing concentration of CuO NPs. This stability in the Type I: Type II ratio may be an indicator of clastogenic effects however it should be mentioned that total number of micronucleus counted was not sufficient to distinguish with certainty between aneugenic and clastogenic

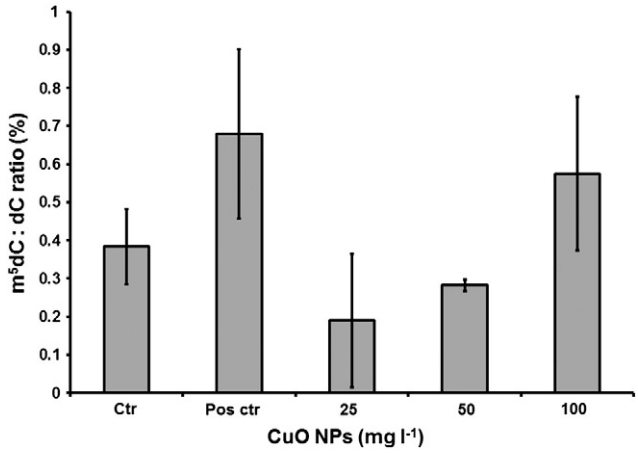

Fig. 6. Change in the ratio $m^5dC/(dC + m^5dC)$ in DNA extracts of N2A cells after a 24 h exposure to 12.5, 25, 50 and 100 mg l^{-1} CuO NPs. Cyclophosphamide was used as a positive control (Pos Ctr). Data are presented as mean ± standard deviation (n = 3).

effect of CuO NPs using the micronucleus size-classification approach (Hashimoto et al., 2010).

4. Discussion

CuO NPs were previously identified as highly toxic with effects on cell viability, cellular oxidative balance and DNA integrity (Karlsson, 2010; Ahamed et al., 2010; Wang et al., 2011). The genotoxic effect of CuO NPs is considered to be mainly attributed to the nanoparticulate form and not to the presence of soluble copper ions (Karlsson, 2010; Wang et al., 2012). However, several aspects of the genotoxicity of CuO NPs still remained to be investigated. In this study, we further investigated the genotoxic effects of CuO NPs using the N2A mouse neuroblastoma cell lines.

When N2A cells were exposed to CuO NPs, a decrease of cell viability was observed after 24 h of treatments. However, at the highest concentration tested (400 mg l^{-1}) cell viability was still 63.1% of the control value, indicating that N2A cells are not very sensitive to CuO NP effects compared to other *in vitro* cell cultures. For the human cell lines THP-I and A549, the concentrations inducing a 50% decrease of cell viability for a 24 h treatment to 45 nm CuO NPs were between 3.89 and 31.07 mg l^{-1} (Lanone et al., 2009). Ahamed et al. (2010) indicated a 48% decrease of cell viability, using the MTT assay, in A549 cells exposed to 50 mg l^{-1} CuO NPs of 65 nm. The differences in the toxic response of N2A cells compared to THP-I and A549 cells may be associated with cellular differences (membrane composition, number of mitochondria) due to their origin, phenotype or cellular function (Watanabe et al., 2002; Souid-Mensi et al., 2008). The lower sensitivity of N2A cells may also be caused by the different agglomeration states of CuO NPs in the culture media. The N2A culture medium has a high ionic strength and contains several types of protein, amino acids or glucose molecules that can be adsorbed on the NP surface (Amirnasr et al., 2011; Monopoli et al., 2011; Joshi et al., 2012). Change of NP surface properties induced by the interaction with the culture medium may influence the physicochemical properties and therefore the toxicity of nanomaterials (Mukherjee et al., 2010). In the culture medium of A549 cells, Ahamed et al. (2010) found a particle hydrodynamic diameter of 65.59 nm for CuO NPs having an initial particle diameter of 50–60 nm, while CuO NPs having an initial particle diameter of 70–100 nm were found to have a hydrodynamic diameter of 307 nm in the N2A culture medium. These complexes may be hypothesized to be due to the binding of albumin, which was used for particles stabilisation (Bihari et al., 2008), to form a protein corona at the CuO NP surface. The presence of such protein corona may have a significant impact on its biological effect (Monopoli et al., 2011). In addition, agglomeration of CuO NPs in the media increase the particle size above the nanometer range (1–100 nm), thus reducing the surface specific effects that are associated with the nanometer range. Under those conditions, solubilisation of the particles may have a more important effect compared to previous findings (Karlsson, 2010; Wang et al., 2012). Solubilisation of CuO NPs into Cu^{2+} was found to be the most important process for A549 cells exposed to CuO NPs (Hanagata et al., 2011). Therefore, for N2A cells exposed to an agglomerated form of CuO NPs, the contribution of the soluble Cu^{2+} fraction can be hypothesized to be more important.

Toxic effect of CuO NPs at the cellular level was previously characterized by the generation of oxidative stress and DNA damage (Karlsson, 2010; Ahamed et al., 2010; Wang et al., 2012). However, such aspects of CuO NP toxicity are still to be investigated in other cell lines beside A549, which is a heterogeneous cell line with multiple phenotypes presenting different levels of toxicological sensitivity (Watanabe et al., 2002). The genotoxicity of CuO NPs was therefore evaluated in N2A cells using different assays to characterize the DNA alterations induced by CuO NPs. Our results indicate that CuO NPs can induce both oxidative stress and DNA fragmentation in N2A cells at a concentration of 25 mg l^{-1}. At this concentration, cell viability was 85% of the control value. Oxidative stress is often considered as the primary mechanisms

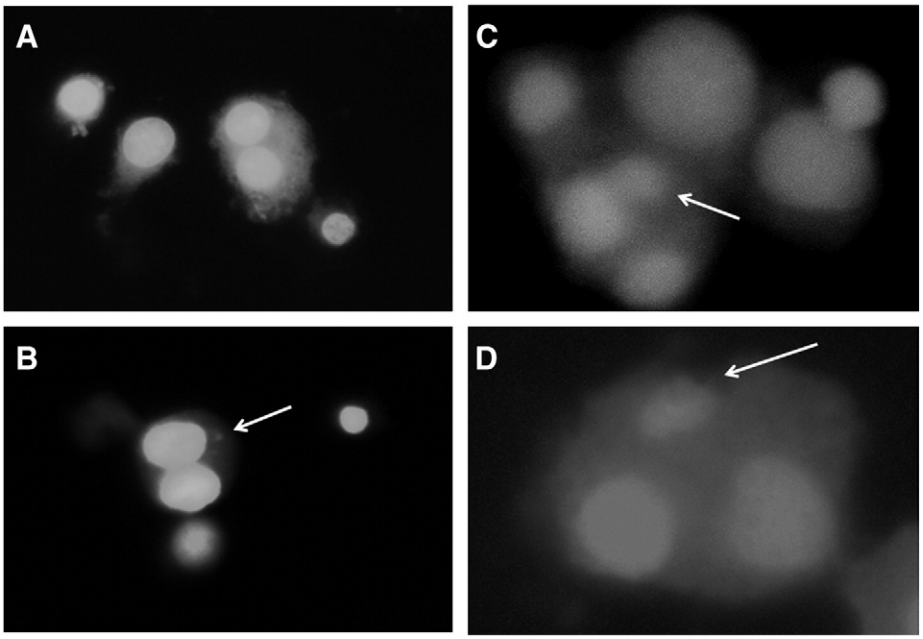

Fig. 7. Examples of control (A) and micronucleated cells (B, C, D) for N2A cells.

of NP toxicity (Nel et al., 2006; Shukla et al., 2011). Treatment of A549 cells to CuO NPs resulted in MDA formation, activation of antioxidant enzymes and increased expression of the DNA repair proteins p53 and Rad51 (Ahamed et al., 2010). In this report, the authors hypothesized that genotoxicity of CuO NPs may be mediated *via* oxidative stress and lipid peroxidation. In our study, DNA fragmentation and MDA formation were found significantly at the same concentration (25 mg l^{-1}). However, DNA fragmentation can also be induced by several cellular processes, such as necrosis and apoptosis, therefore a complementary approach to evaluated the genotoxic effect of CuO NPs was used.

Micronucleus formation may be caused by an alteration of DNA integrity which results in small chromosome fragments (castogenic effect) or by an alteration of mitotic processes which results in an abnormal number of chromosomes (aneugenic effect) (Kirsch-Volders et al., 2011). The formation of micronuclei in N2A cells exposed to CuO NPs may therefore be an indicator of structural alteration of DNA. Our results indicate a predominance of Type I micronuclei, which are an indicator of a clastogenic effect. These results are in agreement with the DNA fragmentation assay and confirm the genotoxic effect of CuO NPs in N2A cells. The increase of micronucleus formation induced by CuO NPs was found to be low compared to other clastogenic compounds such as methyl methanesulfonate, N-methyl–N′-nitro–N–nitroso-guanidine and mitomycin C, which increased micronucleus frequency up to more than 300 micronuclei per 1000 binucleated cells (Matsushima et al., 1999). The induction of micronucleus formation by CuO NPs in N2A cells was also lower than for TiO_2 NPs in human lymphocytes (Kang et al., 2008) but higher than for C_{60} NPs, SiO_2 NPs and Ag NPs in hamster, mouse and human cells, respectively (Shinohara et al., 2009; Park et al., 2011; Li et al., 2012). Therefore, CuO NPs may be considered as a genotoxic nanomaterial compared to other NPs.

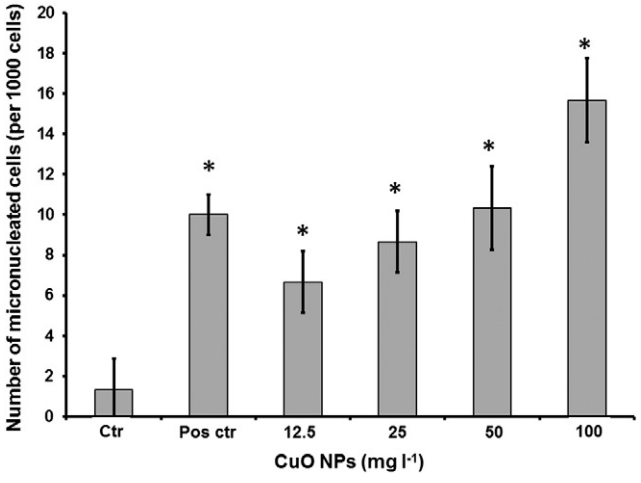

Fig. 8. Micronucleus count in N2A cells after a 24 h exposure to 12.5, 25, 50 and 100 mg l^{-1} CuO NPs. Cyclophosphamide was used as a positive control (Pos Ctr). Data are presented as mean ± standard deviation (n = 3).

The micronucleus assay was the most sensitive approach to evaluate the toxic effects of CuO NPs in N2A cells. Indeed, at 12.5 mg l^{-1} CuO NPs, the micronucleus frequency was already 5 times the negative control value while cell viability was not significantly changed compared to control value ($p = 0.99$). Our results indicate that, similarly to TiO_2 and SiO_2 NPs, micronucleus formation induced by CuO NPs in N2A cells occurs at lower concentration than cytotoxicity, oxidative stress or DNA fragmentation (Rahman et al., 2002; Wang et al., 2007). Recently, it was shown that the genotoxic effect of CuO NPs, in conditions where CuO NPs were less agglomerated and soluble copper effect was low, is due to the formation of reactive oxygen species (Wang et al., 2012). Under our conditions CuO NPs formed large (over 300 nm) agglomerates in the culture medium and genotoxic effects were observed at lower concentrations than lipid peroxidation induced by oxidative stress. This may indicate a different mode of action for small compared to larger CuO NP agglomerates and this effect may be due to a more important contribution of the soluble copper fraction under our conditions. The contribution of particle solubilisation, both in the media and inside the cell (Trojan Horse effect), will have to be determined in order to provide a better understanding of the genotoxic potentials of CuO NPs at the cellular level.

5. Conclusions

In this study, the toxic effects of CuO NPs were investigated in N2A cells to provide a better understanding of the toxicological risks of CuO NPs in future nanotechnology developments. N2A cells were found to be less sensitive to CuO NP effects than other *in vitro* cultured cells. This lower sensitivity may be due to the agglomeration of CuO NPs

in the culture media, which resulted in an average particle size over 300 nm. Agglomeration of CuO NPs reduces surface-specific effects specific to nano-scale materials and increases the contribution of particle solubilisation in the toxic response induce to N2A cells. Agglomerated CuO NPs were found to induce both cytotoxic and genotoxic effects in N2A cells. Significant genotoxic effects were observed at a concentration of 12.5 mg l^{-1}, where no decrease of cell viability was found. Considering that the NP fraction reaching the brain *in vivo* only accounts for less than 0.02% of total administrated dose, the risk of neurotoxicity of CuO NPs may be less important than for other organs, such as the liver, that accumulate an higher amount of NPs (Lasagna-Reeves et al., 2010; Xie et al., 2011). However, considering the importance of genotoxic effect in the development of cancer, the risk of CuO NPs should be investigated in order to ensure a safe development of CuO-based nanomaterials. Further research will aim on the contribution of particle solubilisation in CuO NP toxicity and the clarification of the nature of the genotoxic effect induced by CuO NPs.

Acknowledgments

This work was supported by research grants awarded to W.G. Matias by the Conselho Nacional de Desenvolvimento Científico e Tecnológico (Brazil), and to R. Popovic by the Natural Sciences and Engineering Research Council (Canada). F. Perreault was supported by a mobility fellowship from the Ministère de l'Éducation, des Loisirs et du Sport du Québec for his work in the LABTOX.

References

Ahamed M, Siddiqui MA, Akhtar MJ, Ahmad I, Pant AB, Alhadla HA. Genotoxic potential of copper oxide nanoparticles in human lung epithelial cells. Biochem Biophys Res Commun 2010;396:578–83.
Amirnasr A, Emtiazi G, Abasi S, Yaaghoobi M. Adsorption of hemoglobin, fatty acid and glucose to iron nanoparticles as a mean for drug delivery. J Biochem Tech 2011;3:280–3.
Bihari P, Vippola M, Schultes S, Praetner M, Khandoga AG, Reichel CA, et al. Optimized dispersion of nanoparticles for biological in vitro and in vivo studies. Part Fibre Toxicol 2008;5:1-14.
Bradford MM. A rapid and sensitive method for the quantification of microgram quantities of protein utilizing the principle of protein dye. Anal Biochem 1976;72:248–54.
Chen J, Zhu J, Cho H-H, Cui K, Li F, Zhou X, et al. Differential cytotoxicity of metal oxide nanoparticles. J Exp Nanosci 2008;3:321–8.
Dastjerdi R, Montazer M. A review on the application of inorganic nanostructured materials in the modification of textiles: focus on antimicrobial properties. Colloids Surf B Biointerfaces 2010;79:5-18.
Delgado K, Quijada R, Palma R, Palza H. Polypropylene with embedded copper metal or copper oxide nanoparticles as a novel plastic antimicrobial agent. Lett Appl Microbiol 2011;53:50–4.
Fenech M. The in vitro micronucleus technique. Mutat Res Fundam Mol Mech Mugag 2000;455:81–95.
Gonzalgo ML, Jones PA. Mutagenic and epigenetic effects of DNA methylation. Mutat Res 1997;386:107–18.
Hanagata N, Zhuang F, Connolly S, Li J, Ogawa N, Xu M. Molecular responses of human lung epithelial cells to the toxicity of copper oxide nanoparticles inferred from whole genome expression analysis. ACS Nano 2011;27:9326–38.
Hashimoto K, Nakajima Y, Matsumura S, Chatani F. An in vitro micronucleus assay with size-classified micronucleus counting to discriminate aneugens from clastogens. Toxicol In Vitro 2010;24:208–16.
Humpage AR, Ledreux A, Fanok S, Bernard C, Briand JF, Eaglesham G, et al. Application of the neuroblastoma assay for paralytic shellfish poisons to neurotoxic freshwater cyanobacteria: interlaboratory calibration and comparison with other methods of analysis. Environ Toxicol Chem 2007;26:1512–9.
Jensen KA, Kembouche Y, Christiansen E, Jacobsen NR, Wallin H, Guiot C, et al. Final protocol for producing suitable manufactured nanomaterial exposure media. NANOGENOTOX report n°3; 2011. July :34 pp.
Joshi S, Ghosh I, Pokhrel S, Madler L, Nau WM. Interactions of amino acids and polypeptides with metal oxide nanoparticles probed by fluorescent indicator adsorption and displacement. ACS Nano 2012;6:5668–79.
Kang SJ, Kim BM, Lee YJ, Chung H. Titanium dioxide nanoparticles trigger p53-mediated damage response in peripheral blood lymphocytes. Environ Mol Mutagen 2008;49: 399–405.
Karlsson HL. The comet assay in nanotoxicology research. Anal Bioanal Chem 2010;298: 651–66.
Karlsson HL, Cronholm P, Gustafsson J, Moller L. Copper oxide nanoparticles are highly toxic: a comparison between metal oxide nanoparticles and carbon nanotubes. Chem Res Toxicol 2008;21:1726–32.
Kirsch-Volders M, Plas G, Elhajouji A, Lukamowicz M, Gonzalez L, Loock KV, et al. The in vitro MN assay in 2011: origin and fate, biological significance, protocols, high throughput methodologies and toxicological relevance. Arch Toxicol 2011;85:873–99.
Kouadio JH, Danob SD, Moukha S, Mobio TA, Creppy EE. Effects of combinations of Fusarium mycotoxins on the inhibition of macromolecular synthesis, malondialdehyde levels, DNA methylation and fragmentation, and viability in Caco-2 cells. Toxicon 2007;49:306–17.
Lanone S, Rogerieux F, Geys J, Dupont A, Maillot-Marechal E, Boczkowski J, et al. Comparative toxicity of 24 manufactured nanoparticles in human alveolar epithelial and macrophage cell lines. Part Fibre Toxicol 2009;6:14.
Lasagna-Reeves C, Gonzalez-Romero D, Barria MA, Olmedo I, Clos A, Sadagopa Ramanujam VM, et al. Bioaccumulation and toxicity of gold nanoparticles after repeated administration in mice. Biochem Biophys Res Commun 2010;393: 649–55.
Li F, Zhou X, Zhu J, Ma J, Huang X, Wong STC. High content image analysis for human H4 neuroglioma cells exposed to CuO nanoparticles. BMC Biotechnol 2007;7:66.
Li Y-F, Chen C. Fate and toxicity of metallic and metal-containing nanoparticles for biomedical applications. Small 2011;7:2965–80.
Li Y, Chen DH, Yan J, Chen Y, Mittelstaedt RA, Zhang Y, et al. Genotoxicity of silver nanoparticles evaluated using the Ames test and in vitro micronucleus assay. Mutat Res 2012;745:4-10.
Marnett LJ. Lipid peroxidation—DNA damage by malondialdehyde. Mutat Res Fundam Mol Mech Mugag 1999;424:83–95.
Matias WG, Creppy EE. 5-Methyldeoxycytosine as a biological marker of DNA damage induced by okadaic acid in Vero cells. Environ Toxicol Water 1998;13:83–8.
Matsushima T, Hayashi M, Matsuoka A, Ishidate Jr M, Miura KF, Shimizu H, et al. Validation study of the in vitro micronucleus test in a Chinese hamster lung cell line (CHL/IU). Mutagenesis 1999;14:569–80.
Monopoli MP, Walczyk D, Campbell A, Elia G, Lynch I, Bombelli FB, et al. Physical–chemical aspects of protein corona: relevance to *in vitro* and *in vivo* biological impacts of nanoparticles. J Am Chem Soc 2011;133:2525–34.
Mukherjee SP, Davoren M, Byrne HJ. In vitro mammalian cytotoxicological study of PAMAM dendrimers—towards quantitative structure activity relationships. Toxicol In Vitro 2010;24:1169–77.
Nel A, Xia T, Madler L, Lin N. Toxic potential of materials at the nano-level. Science 2006;311:622–7.
Oszlanczi G, Vezer T, Sarkozi L, Horvath E, Konya Z, Papp A. Functional neurotoxicity of Mn-containing nanoparticles in rats. Ecotoxicol Environ Saf 2010;73:2004–9.
Ouanes Z, Abid S, Ayed I, Anane R, Mobio T, Creppy EE, et al. Induction of micronuclei by Zearalenone in Vero monkey kidney cells and in bone marrow cells of mice: protective effect of vitamin E. Mutat Res 2003;538:63–70.
Park MVDZ, Verharen HW, Zwart E, Hernandez LG, Benthem JV, Elsaesser A, et al. Genotoxicity evaluation of amorphous silica nanoparticles of different sizes using the micronucleus and the plasmid lacZ gene mutation assay. Nanotoxicology 2011;5:168–81.
Peralta-Videa JR, Zhao L, Lopez-Moreno ML, de la Rosa G, Hong J, Gardea-Torresdey JL. Nanomaterials and the environment: a review for the biennium 2008–2010. J Hazard Mater 2011;186:1-15.
Perreault F, Matias MS, Melegari SP, Carvalho Pinto CRS, Creppy EE, Popovic R, et al. Investigation of animal and algal bioassays for reliable saxitoxin ecotoxicity and cytotoxicity risk evaluation. Ecotoxicol Environ Saf 2011;74:1021–6.
Rahman Q, Lohani M, Dopp E, Pemsel H, Jonas L, Weiss DG, et al. Evidence that ultrafine titanium dioxide induces micronuclei and apoptosis in Syrian hamster embryo fibroblasts. Environ Health Perspect 2002;110:797–800.
Ren G, Hu D, Cheng EWC, Vargas-Reus MA, Reip P, Allaker RP. Characterisation of copper oxide nanoparticles for antimicrobial applications. Int J Antimicrob Agents 2009;33: 587–90.
Sebaugh JL. Guidelines for accurate EC50/IC50 estimation. Pharm Stat 2010;10:128–34.
Sharma HS, Hussain S, Schlager J, Ali SF, Sharma A. Influence of nanoparticles on blood-brain barrier permeability and brain edema formation in rats. Acta Neurochir Suppl 2010;106:359–64.
Shinohara N, Matsumoto K, Endoh S, Maru J, Nakanishi J. In vitro and in vivo genotoxicity tests on fullerene C60 nanoparticles. Toxicol Lett 2009;191: 289–96.
Shukla RK, Sharma V, Pandey AK, Singh S, Sultana S, Dhawan A. ROS-mediated genotoxicity induced by titanium dioxide nanoparticles in human epidermal cells. Toxicol In Vitro 2011;25:231–41.
Singh N, Manshian B, Jenkins GJS, Griffiths SM, Williams PM, Maffeis TGG, et al. NanoGenotoxicology: the DNA damaging potential of engineered nanomaterials. Biomaterials 2009;30:3891–914.
Skocaj M, Filipic M, Petkovic J, Novak S. Titanium dioxide in our everyday life; is it safe? Radiol Oncol 2011;45:227–47.
Slade D, Lindner AB, Paul G, Radman M. Recombination and replication in DNA repair of heavily irradiated *Deinococcus radiodurans*. Cell 2009;136:1044–55.
Souid-Mensi G, Moukha S, Mobio TA, Maaroufi K, Creppy EE. The cytotoxicity and genotoxicity of okadaic acid are cell-line dependent. Toxicon 2008;51: 1338–44.
Tinwell H, Ashby J. Micronucleus morphology as a means to distinguish aneugens and clastogens in the mouse bone marrow micronucleus assay. Mutagenesis 1991;6: 193–8.
Tsoli M, Kuhn H, Brandau W, Esche H, Schmid G. Cellular uptake and toxicity of Au_{55} clusters. Small 2005;1:841–4.
Wang JJ, Sanderson BJS, Wang H. Cytotoxicity and genotoxicity of ultrafine crystalline SiO_2 particulate in cultured human lymphoblastoid cells. Environ Mol Mutagen 2007;48:151–7.

Wang Y, Aker WG, Hwang H-M, Yedjou CG, Yu H, Tchounwou PB. A study of the mechanism of in vitro cytotoxicity of metal oxide nanoparticles using catfish primary hepatocytes and human HepG2 cells. Sci Total Environ 2011;409:4753–62.
Wang Z, Li N, Zhao J, White JC, Qu O, Xing B. CuO nanoparticle interaction with human epithelial cells: cellular uptake, location, export, and genotoxicity. Chem Res Toxicol 2012;25:1512–21.
Watanabe N, Dickinson DA, Krzywanski DM, Iles KE, Zhang H, Venglarik CJ, et al. A549 subclones demonstrate heterogeneity in toxicological sensitivity and antioxidant profile. Am J Physiol Lung Cell Mol Physiol 2002;283:L726–36.
Xie G, Wang C, Sun J, Zhong G. Tissue distribution and excretion of intravenously administered titanium dioxide nanoparticles. Toxicol Lett 2011;205:55–61.
Zhivotosky B, Orrenius S. Assessment of apoptosis and necrosis by DNA fragmentation and morphological criteria. Curr Protoc Cell Biol 2001;18. Unit 18.3.
Zukiel R, Nowak S, Barciszewska A-M, Gawronska I, Keith G, Barciszewska MZ. A simple epigenetic method for the diagnosis and classification of brain tumors. Mol Cancer Res 2004;2:196–202.